

General Disclaimer

One or more of the Following Statements may affect this Document

- This document has been reproduced from the best copy furnished by the organizational source. It is being released in the interest of making available as much information as possible.
- This document may contain data, which exceeds the sheet parameters. It was furnished in this condition by the organizational source and is the best copy available.
- This document may contain tone-on-tone or color graphs, charts and/or pictures, which have been reproduced in black and white.
- This document is paginated as submitted by the original source.
- Portions of this document are not fully legible due to the historical nature of some of the material. However, it is the best reproduction available from the original submission.

Trade names or manufacturers' names are used in this report for identification only. This usage does not constitute an official endorsement, either expressed or implied, by the National Aeronautics and Space Administration.

MECHANICAL PROTECTION OF DLC FILMS ON FUSED SILICA SLIDES

Dan Nir*
National Aeronautics and Space Administration
Lewis Research Center
Cleveland, Ohio 44135

SUMMARY

Measurements were made with a new test for improved quantitative estimation of the mechanical protection of thin films on optical materials. The mechanical damage was induced by a sand blasting system using spherical glass beads. Development of the surface damage was measured by the changes in the specular transmission and reflection, and by inspection using a surface profilometer and a scanning electron microscope. The changes in the transmittance versus the duration of sand blasting was measured for uncoated fused silica slides and coated ones. It has been determined that the diamondlike carbon films double the useful optical lifetime of the fused silica. Theoretical expressions were developed to describe the stages in surface deterioration. Conclusions were obtained for the SiO_2 surface removal mechanism and for the film removal mechanism.

INTRODUCTION

Fused silica, like other brittle materials, is damaged by the impact of round objects causing the formation of Hertz cone cracks. This type of damage has been extensively investigated (ref. 1). Single impact damage of liquid drops and solid particles on brittle materials has also been discussed recently (refs. 2 to 4). One can use these references to calculate erosion rates and elastic stress distributions. There are also indications of the dependence of erosion rates on particle size (refs. 3 and 5). The progression of material removal has been investigated by Adler (ref. 6) who proposed a model for the mechanism. This model suggests the formation of a pit by the crossing of 3 Hertz cones.

Most investigations measure the erosion at a steady rate under certain conditions, and sometimes relate them to a specified parameter. There is a great interest in the investigation of the initial stage of surface damage and the beginning of material removal.

The mechanical protection of thin films on brittle materials is not well known. Recent calculations by Mathewson (ref. 7) suggest that soft films may reduce surface damage by reducing the maximum stress. His work also suggests damage reduction by hard films. The mechanical properties of a steel substrate, ion plated with lead, was investigated by Elsherbini and Halling (ref. 8) using the capacitance method. The behavior of the coated steel at film thicknesses between 1 and 15 μm was consistent with model predictions based on the elastic Hertz stress distribution. At a film thickness of 15 μm the micromechanical behavior was similar to that of bulk lead.

*NRC-NASA Research Associate.

The scratch and abrasion tests used to evaluate the protection afforded by thin films depend on adhesion and do not give accurate estimates of the increased endurance of the optical material in the actual application environment.

This paper reports the behavior of coated and uncoated fused silica evaluated at early stages of surface damage. The damage is induced by spherical glass beadblasting. The optical performance is evaluated by measurement of the specular transmittance and reflectance. This method was found to be sensitive to surface damage even before material was removed. The evolution of optical degradation with respect to the duration of beadblasting for fused silica coated with hard diamondlike carbon films was measured and compared to that of uncoated fused silica.

APPARATUS AND PROCEDURE

Beadblasting System

An industrial sandblasting machine, TRINCO 40"x26"/600, was used for the experiments. Pressure controlled air accelerated new KREBER 810-220 glass beads which were put into the machine at the beginning of the series of beadblast exposures. The glass beads were 100(15) μm diameter spheres (fig. 1). The geometry of the beadblast gun and the substrate were fixed by mechanical clamps to within 1 mm accuracy. The substrate was located 20 cm axially downstream of the gun. Two by 2 by 0.2 cm fused silica slides were used as the substrates. They were beadblasted under various experimental conditions. Half of the fused silica was masked during beadblasting by Kapton® adhesive tape to enable the relative comparison of the features of both halves.

Stability of the Gun

The commercial sandblasting machine utilized was not designed for precise experimentation. The pressure regulator was not of high accuracy, and had to be left in the same position during the series of experiments for reasonable repeatability. The mass of beadblast particles was found to have only a slight dependence on the blast pressure (fig. 2). The blasted beads were collected over large areas when the gun and the sample were covered by metal sheets. Additional dishes were put in other places along the blast chamber and the collected particles were weighted. It was shown that 80 to 90 percent of the glass beads were collected by this procedure.

The stability of the bead flow with time and its reproducibility was also checked. In most of the tests the bead weight was proportional to the duration, but in a few cases deviations of up to 20 or 30 percent were observed. The total mass of the beads was the parameter which better characterized the time evolution of damage.

The spatial profile of the beadblast damage in the transverse direction was determined by the spatial dependence of the optical features of the beadblasted fused silica substrate. Figure 3 shows the optical transmittance, of a fused silica substrate after blasting at a pressure of 10^5 Pa plotted against the position of the sample in the horizontal and vertical directions.

The damage distribution at this pressure is almost flat, therefore the optical results do not depend on the position. At pressures higher than 1.5×10^5 Pa the distribution is not flat and there is more damage in the center of the sample.

Velocity of the Sand

The glass bead velocity was measured in a way similar to reference 9. The particle stream was further collimated by an aperture 10 by 5 mm at a distance of 12 cm from the gun. A rotating disk was placed 17 cm downstream and had apertures of 4.5 mm in diameter at a radius of 77 mm. Twenty centimeters behind and attached to the disk, a glass substrate was firmly mounted. The system was initially operated at a very low rotation speed and an image of damaged glass was formed. The motor was then operated at the regular rotation speed of 1720 rpm and a second image of damage was formed on the same glass substrate. The velocity was then calculated from the shift of the image.

Figure 4 shows the square of the bead velocity as a function of the air pressure of the beadblasting system. The relation is linear over a wide range. Under 0.5×10^5 Pa there is no particle ejection from the gun.

The above relation could be expected from the following considerations. The gas velocity has a similar linear relationship with the pressure as predicted by the Bernoulli principle and measured by reference 9. The Stokes' viscosity force on the round beads is proportional to the relative velocity. The glass bead velocity is a small fraction of the gas velocity, and the force is approximately constant during the ejection of the beads. The deceleration outside the gun by the viscous drag in air is proportional to the velocity of the beads and is small. Therefore, the bead velocity is expected to have this linear relationship with the pressure. The relation can be interpreted as the transfer of the work of the pressure on the bead into kinetic energy.

Optical Measurements

Optical transmittance measurements were made by adapting an Ellipsometer II system from Applied Material Inc. The narrow light beam from a He-Ne laser ($\lambda = 6328$ Å) at 70° was passed through the sample then reflected at 70° from the surface normal of a 7.1 cm diameter Si wafer, into the 4 mm collimator of a photomultiplier detector. The polarization aspects of the ellipsometer were not utilized. The sample was mounted perpendicularly to the beam between the laser and Si wafer, with the beam incident upon the damaged area to allow diffuse scattering by the damaged surface. The specularly transmitted light intensity through the damaged area was compared to that through the undamaged area. This ratio normalizes the effects of surface reflections and bulk absorptions of the substrate, but does not eliminate effects due to the diffuse scattering of the damaged surface. The laser was stable up to a few percents. The linearity between the light intensity and the output current of the photomultiplier tube was found to be proportional, as verified by comparison of the detector output with the short circuit current of a solar cell. The measurements on the same samples yielded transmittance values equal within the experimental errors of 3 percent.

The mirror for the reflection of the beam was a Si wafer which has a high index of refraction. The fixed reflection angle of the ellipsometer (70°) is still far from the Brewster polarizing angle. Systematic transmittance measurements were taken on a sample when both the polarizer and analyzer positions were independently changed in relation to the beam and the reflecting mirror. The transmittance results were independent of the polarizer and analyzer positions up to 5 percent.

The optical measurements of coated fused silica samples were made in the following way. During the diamond like carbon (DLC) deposition, half of the fused silica sample was masked with Kapton[®] adhesive tape thus allowing deposition on only half of the sample. During the beadblasting the sample was again protected by Kapton[®] tape in such a way that half of the coated and half of the uncoated regions were exposed. In this arrangement four regions, each a quarter of a slide, were obtained - plain silica, coated silica, uncoated-beadblasted silica, coated-beadblasted silica. By comparison of the transmittance and reflectance over the various regions, one can extract the optical effect of a coating as well as the protection it provides. In this way, the substrate reflection, absorption and variations between slides were cancelled out.

The loss in specular reflectance due to beadblasting was determined by replacing the Si wafer with a fused silica substrate, with the damaged area to the upper side. Reflectance measurements were found to be more sensitive to polarization and other sources of error, therefore giving less reproducible results. The reflectance measurements were important in evaluating DLC film, because the film absorbs light and the removal of the film from the fused silica may result in enhancement of the transmittance.

Surface Measurements

The protective film thickness and the roughness of the surface were measured by a Tencor α -step[®] surface profilometer. The profile measuring stylus utilizes a diamond tip having a radius of curvature of $12.5\ \mu\text{m}$ and is loaded to a contact force of 50 mg. The profilometer can resolve vertical variations to less than 100 Å, but will not sense grooves narrower than the stylus diameter. The system can calibrate the height by a flat area near the measured region and resolve surface risings from grooved areas. The surfaces were also examined by both an optical microscope and a scanning electron microscope to observe the damage patterns.

EXPERIMENTAL RESULTS OF UNCOATED FUSED SILICA

Figure 5 shows the dependence of the beadblast damage on the pressure of the compressed air in the beadblast gun. The damage rate shown is the time rate of the change of specular transmittance, $(-dT/dt)$. The dependence on pressure is strong and all other effects are of secondary importance.

The beadblast damage was found in figure 5 to be exponentially rising with increasing pressure. At the higher pressures of $5 \times 10^5\ \text{Pa}$ the damage rate is two orders of magnitude faster than at the low pressure of $1 \times 10^5\ \text{Pa}$, therefore within a few seconds the transmittance is drastically reduced. Since figure 2 has shown that the quantity of blasted beads has only a slight

dependence upon pressure, it is the damage per particle that changes exponentially with pressure. Figure 4 indicates the relationship between the velocity of the particles and the pressure. Thus, the damage to the surface increases exponentially with the energy of the projectile.

Figure 6 shows typical damage evolution with time at a fixed beadblast pressure of 1.2×10^5 Pa. In this experiment the sand was also collected and its quantity was found to be proportional to the time of beadblasting. Small differences appeared at 8 and 9 min only. Indicated in this figure is the transmittance evolution during blasting for a single sample and the additive transmittance effect of two or more samples versus the combined beadblasting duration. In the case of the combined effect, there may be some contribution of combined scattering but no individual severe damage, because each sample was blasted for less than 5 min. In figure 6, one observes a clear departure between these curves. One also observes that the transmittance reductions are exponential decays which can be extrapolated to lower times. The extrapolation of the long blast durations of single samples crosses the line of 100 percent transmittance at about 4 min. Therefore, this is the incubation time of the process since beadblasting is not expected to cause surface damage before this time. The additive data shows slower damage rates and the estimated incubation time from extrapolation is about 1 min.

Figure 7 shows typical roughness data taken by the surface profilometer. There seems to be two kinds of effects. One is dominant in short times and causes damage that its profile protrudes above the virgin fused silica surface up to about 1000 Å. The other is dominant at long times and causes surface recession as well as roughening.

Figure 8 shows SEM photographs which indicate other aspects of the damage process. The photographs were taken on the samples described in figure 7. At 2 min there are only a few Hertzian cone cracks visible. Yet in figure 7(a) there are significant profiles of protrusions above the virgin surface. At 5 min of beadblasting, some substrate material flakes are thrown out. These flakes have odd shapes and are thrown out from the regions between two or more close Hertzian cracks. At 8 min the damaged area appears as a ring around the area compressed by the impacting glass beads. The failed area is of the same approximate size as the glass beads.

EXPERIMENTAL RESULTS OF DLC COATED FUSED SILICA

Time Evolution of Specular Transmittance and Reflectance

The transmittance of the four quadrants (uncoated, not beadblasted; coated, not beadblasted; uncoated, beadblasted; coated, beadblasted) of the samples were measured in the ellipsometer and the reduction in transmittance due to the damage was extracted. The specular transmittance values of the beadblasted regions were divided by the values of the regions which were not beadblasted to yield the normalized transmittance, which cancels out many substrate, film and beadblasting errors.

Figure 9 shows us the normalized transmittance versus duration of beadblast for 1000 Å films blasted at a pressure of 10^5 Pa. At this pressure and at a blasting distance of 20 cm, the sand velocity is about 30(2) m/sec. The lower curve of figure 9 is similar to figure 6, and shows the damage

evolution of uncoated fused silica. The upper curve is the normalized transmittance of the beadblasted DLC film. One observes the protection effects of the DLC film by the slower degradation of the optical transmittance. Films at thicknesses of 500 to 3000 Å, which were beadblasted by a pressure of $1.0\text{--}1.5 \times 10^5$ Pa, showed similar behavior.

Figure 10 shows the specular reflectance versus the beadblast duration for the same samples as in figure 9. In this figure there are two distinct curves which demonstrates the film protection effect.

Protection Curve

The transmittance and reflectance data in figures 9 and 10 can be combined in a form which eliminates some experimental errors. Plotting the transmittance through the beadblasted film versus the transmittance in the beadblasted, uncoated fused silica cancels out all time dependence, sand flow rate variations, etc. Figure 11 shows this presentation. The experimental curve should pass through two points. One is the 100 percent transmittance ratio of two samples prior to beadblasting, and the second is the residual transmittance ratio in both samples (about 5 percent) after the film is removed and the surface collapsed. The protection effect of the film is demonstrated by the deviation of experimental points from a 45° line through the origin. A quantitative way to describe the protection is by the slope of the experimental curve near 100 percent transmittance which gives the extension of lifetime in the high optical performance region. The small difference between transmittance and reflectance will be discussed later.

Surface Profiles

Figure 12 compares the surface roughness of coated and uncoated samples blasted for various durations. The upper curves show the surface profile of the of uncoated, beadblasted fused silica. The lower curves show the roughness of the beadblasted regions with 1000 Å DLC coating. These profiles indicate the roughness of the uncoated regions is higher than that of the coated ones. The pronounced protection effect is shown as a reduction in the number of protrusions above the virgin surface which is dominant at short times. The protection effect can also be seen in the reduction of the number of pits. These pits, from which material is thrown when 3 Hertz cones cross each other, represent the dominant surface removal process at longer times. Inspection of the damage in coated fused silica under the optical microscope does not show any essential difference in the process but only in the evolution rate. The damage in coated fused silica is similar to that of an uncoated one which is beadblasted for a shorter duration.

COMPARISON WITH THEORY

Damage Characteristics

The general description of the damage has been given in previous figures. After some beadblasting, round cracks are formed. As expected in a brittle material they are identified as Hertz cones. Their diameter however, is comparable to the diameter of the spherical glass beads (fig. 1), but because the

penetration is small, we get $\Delta A \approx 1/4 \pi R^2$ where ΔA is the impacted area and R is the bead radius. After sufficient beadblast duration some material is thrown out between neighboring Hertz cones. The damage is three overlapping Hertz cone cracks of the area $\Delta A \approx \pi(R)^2$, which is twice the crack dimension. Later the damage is a ring around the impacted region and the ratio of radii is ~ 1.5 , thus we get again $\Delta A \approx 1/2(\pi R^2)$.

These characteristics of the damage are well known. They appear in single impacts at low and high velocities (ref. 1 and ref. 6). They also appear in erosion by liquids of brittle materials (ref. 2). In conclusion, the damage characteristics (not damage rate) are determined by the dimensions of the beads and not by the substrate material.

Beadblast Damage Characteristics

If the jet is ejecting beads of radius R and velocity v , then R is the dimension which characterizes the damage. Particles will give accumulated effect if their impinging positions are less than a distance R apart. Therefore, the accumulated damage depends on the factor which measures the overlapping impacts.

$$K_e = J \cdot t \cdot \frac{1}{4}(\pi R^2) \quad (1)$$

When J is the flux of particles per unit area in the substrate position, t is the beadblast duration, and R is the radius of the beads. It should be emphasized that K_e depends on geometry of the experiment and the properties of the sandblasting system and the beads, but not on the substrate material itself.

Behavior of Fused Silica Subjected to Beadblasting

The value of K_e in eq. (1) can be calculated in the following way. The average mass of any bead is about $4/3 \pi R^3 g$ where g is the specific gravity of the glass and its value is 2.65 gr/cm^3 . The mass flow of ejected beads is taken from figure 2, and when divided by the total beadblasted area and by the mass of a single bead it yields an approximate value of J for eq. (1). The value of t in eq. (1) can be estimated from the rate of loss of specular transmittance in figure 5. For every pressure, the beadblast duration can be calculated for which the specular transmittance is reduced to 50 percent, i.e. $-0.5/(dT/dt)$. Introducing all the terms together one obtains an estimate for the overlapping impacts which are needed to reduce the transmittance to 1/2 at any pressure. Let the mass of the sand be M and the rate of flow be $\Delta M/\Delta t$. A is the total area of blast. We then get

$$K_e\left(\frac{1}{2}\right) = \frac{0.5}{\left(-\frac{dT}{dt}\right)} \frac{\left(\frac{\Delta M}{\Delta t}\right)}{\left(\frac{4}{3}\right)\pi R^3 \cdot g} \frac{\pi R^2/4}{A} \quad (2)$$

The number of overlapping impingements on the area $1/4\pi R^2$, which reduces the transmittance to 50 percent is shown in figure 13 and is decreasing exponentially in p . The more peculiar fact, however, is that in reducing the

transmittance to 50 percent, 500 particles at 10^5 Pa are doing the same work as one particle at 5.0×10^5 Pa. The damage itself, however, is in the form of circular Hertz cracks with the dimension $\Delta A = 1/4 \pi R^2$. Regardless of the bead velocity, pits with similar dimensions are formed and material is thrown when 2 or 3 Hertz cracks overlap. At higher damages, a ring of material is thrown around the compressed region of $\Delta A = \pi R^2/4$. A possible explanation for the small dependence on the bead velocity may be that every impact, even in low velocity, leaves some residual damage, D. When the velocity is small a Hertz cone crack is not formed by a single impact, and every impact is mostly in the elastic region. The surface returns to the original position, but some damage, D, still remains. When this damage accumulates and becomes considerable, the surface then cracks and a Hertz cone forms.

Transmittance of Fused Silica Subjected to Beadblasting at High Velocities

When the pressure is high enough, every impinging particle forms a crater and the typical damage area is marked ΔA . Once the area is damaged it scatters the light and no other impingement can flatten the surface. Using the generalized definition of overlapping impacts, K, (like eq. (1)) on typical damage area, one can find mathematical expressions for the transmittance. The probability of having m particles on area ΔA is assumed to be given by the statistical Poisson distribution, which is normalized to 1.0 when summed over m.

$$P(m, K) = e^{-K} \frac{K^m}{m!} \quad (4)$$

And the transmittance is given by the term $m = 0$ which yields the region which has not been impacted.

$$T(K) = e^{-K} \quad (5)$$

Thus, for any process in which typical damage ΔA occurs by single particle impact, this exponential dependence on the blasting duration appears through the parameter K. Plotting this dependence on a semilog scale, a linear dependence on time should be found and the intercept at $t = 0$ is $T = 1.0$. Figure 6 shows that our case is different. Two exponential slopes appear for short and long times and extrapolation of them yield finite times for 100 percent transmittance. These extrapolated times are called incubation times.

Transmittance of Heavily Damaged Fused Silica

It is shown in figures 7 and 8 that when the damage is accumulated some material between Hertz cracks is thrown out. In most cases one can observe three cracks around the thrown flake, but sometimes two or four cracks. A quantitative expression for the damaged area can be derived under the following assumptions: First, any impinging particle is forming a circular crack with the typical area, ΔA , and the number of overlapping cracks on this typical area is given by the Poisson distribution. Second, whenever three cracks partially overlap on ΔA some flakes with area δA are thrown out. This groove with area δA scatters the light completely and further material removal

cannot compensate this scattering. The number of three of overlapping cracks on the area ΔA , with K impingements, is estimated by elementary statistics to be $m(m-1)(m-2)/6$. There is, however, saturation in the effect of the removed material on the scattering.

$$T(m) \approx \left(1 - \frac{\delta A}{\Delta A}\right)^{m(m-1)(m-2)/6} \approx e^{-\delta A/\Delta A \cdot m(m-1)(m-2)/6} \quad (6)$$

Therefore, the combined effect of all particles will give for transmittance

$$T\left(K, \frac{\delta A}{\Delta A}\right) = \sum_{m=0}^{\infty} e^{-K} \frac{K^m}{m!} e^{-\delta A/\Delta A \cdot m(m-1)(m-2)/6} \quad (7)$$

It should be noted that for $m = 0, 1, 2$ the coefficient of $\delta A/\Delta A$ vanishes and these terms give full contribution to transmittance. Figure 14 gives the transmittance versus K for various $\delta A/\Delta A$ values in the region between 0.1 to 0.3. The sensitivity for the parameter $\delta A/\Delta A$ is not large due to the large power of m (eqs. (6) and (7)), and the parameter values are consistent with SEM observations. The dependences for large K , on a semilog scale, are approximately linear. When this line is extrapolated to lower K , the effect of incubation time appears, like the one observed in figure 6. The fit of the model to the measured data (figs. 4, 5, 9, and 10) raises a problem. There is a contradiction between the value of K which is extracted by the model behavior of the transmittance, $K \sim 3$, and K_e calculated in the former section, which is two orders of magnitude bigger. The model is predicting unreasonable results if we use high K values so that $K = K_e$. Initiation of material throwing by three overlapping cracks which is observed in figures 6 to 8, has occurred actually after a high number of overlapping impacts, $K_e = 800$. The discrepancy can be resolved if we remember that not every bead causes a crack. If at some threshold velocity, v_0 , Hertz cone cracks are formed, but no material is thrown, then for lower velocities a factor, $F(v)$, may exist such that F particles at low velocity generate accumulated damage equal to one particle at velocity v_0 .

$$K = K_e/F(v) \quad (8)$$

This value of K should be introduced in expression (7) of the model. The data can be reproduced by further fixing the ratio of the area of the thrown flake to that of the typical crack to the values shown in figure 14, in the region 0.15 to 0.25.

Transmittance for Minimal Surface Damage

The surface profilometer showed that at low pressures of beadblasting and for short exposure times, some parts of the surface seems to protrude above the initial surface. In this case, only small amounts of Hertz cracks are observed. The cracks themselves add one glass-air-glass surface and therefore all of them cannot reduce the transmittance by more than one additional reflection (3 percent in our case). This protrusion above the surface and its forming mechanism are not well understood. The observed profiles at figures 7 and 12 may be partly due to over response of the profiling system. In that case the observed protrusion profiles are images of the roughness of the

surface. The roughness at these low velocities cannot be due to single particle impacts as the Hertz cone cracks at high velocities. The evidence for incubation time at short blast durations shows different dependence of transmission than this of equation (5), and indicates accumulation effects. Moreover, the data of a few consecutive samples in figure 6, in which damage is not accumulated, coincide with the data of single sample at short blast durations. Therefore one may consider an accumulation of optical scattering and not only of material damage (described in the former section). In this proposed model every particle is adding to the roughness or the protrusion over the impacted area ΔA . Parametrization of the resulted light scattering can be done under the following assumptions: The scattering process is done by the change in direction of the normal of the surface at some points. The changes in the normal direction consist of a sum of two small and uncorrelated changes in the x and y directions marked θ_x, θ_y , accordingly. The probabilities of having change θ_x in the normal direction is given by the statistical Gaussian distribution with the second moment θ_0 . θ_y has a similar probability distribution. The light is diffusely scattered when the normal direction is changed by more than θ_c , which is determined by the detector aperture.

The number of impacts, K, over a typical impact area, ΔA , is given by the Poisson distribution, and every impact causes changes in the direction of the normal. Under these assumptions we write

$$T\left(K, \frac{\theta_c}{\theta_0}\right) = 1 - \sum_{m=0}^{\infty} e^{-K} \frac{K^m}{m!} \left[\frac{\iint_{\theta_x^2 + \theta_y^2 > \theta_c^2} d\theta_x d\theta_y e^{-(\theta_x^2 + \theta_y^2)/2m\theta_0^2}}{\iint_0^{\infty} d\theta_x d\theta_y e^{-(\theta_x^2 + \theta_y^2)/2m\theta_0^2}} \right]$$

Changing the integral into polar coordinates, $r^2 = (\theta_x^2 + \theta_y^2)/2m\theta_0^2$ and φ the azimuthal angle, one obtains

$$T\left(K, \frac{\theta_c}{\theta_0}\right) = 1 - \sum_{m=0}^{\infty} e^{-K} \frac{K^m}{m!} \times \left[\left(\frac{\theta_c^2}{2m\theta_0^2} \right) e^{-r^2} 2\pi r dr \right] / \pi \quad (10)$$

and the integral is solved to yield

$$T\left(K, \frac{\theta_c}{\theta_0}\right) = 1 - \sum_{m=0}^{\infty} e^{-K} \frac{K^m}{m!} e^{-\theta_c^2/2m\theta_0^2} \quad (11)$$

Figure 15 shows the dependence of the transmittance on K with $\theta_c^2/2\theta_0^2$ as another parameter.

Although the surface protrusions or roughening and material throwing processes contribute different scattering modes, they are steps of the same surface degradation and figure 6 shows that the behavior changes at $T = 67$ percent. Moreover, the thrown material comes mainly from the more damaged area in which the surface is weaker, and this area is most likely to show protrusion effects. Therefore this area is already scattering the light and the thrown material does not reduce the transmittance much more. We therefore take the predicted transmittance as the minimal value of the two model calculations, and not as any combination of them. We also demand overlapping predictions of the models around $T = 0.67$. In figure 14 one can see that $T = 67$ percent is occurring at about $K \sim 3$, and these results are not sensitive to the exact value of $\delta A/\Delta A$. The observed data at short blasting durations in figure 6 are reproduced by the protrusion model of figure 15 with $\sigma_c^2/2\sigma_0^2 \approx 3$. One can observe in figure 15 that the curves almost overlap when plotted versus the ratio of the two parameters, and the individual values are not important.

Beadblasting Film Removal Mechanism

The mechanism of film removal is very important for the optical damage measurements. The film absorbs a considerable fraction of the laser light and peeling of the films from the flat surface may result in an enhancement of the specular transmittance. The protection curve (fig. 11) may result from this enhancement. Series of reflectance and transmittance measurements have been carried out to exclude this possibility. The polarization angles of the ellipsometer were chosen so that the surface reflectivity of the bare fused silica was once lower, once equal, and once larger than the reflectivity of the coated material. The extracted values of the optical degradation were very close to each other. There was an insignificant difference at very large damages. All the reflectance results were close also to those extracted from the specular transmittance measurements as mentioned in the former sections. This indicates very small, if any, enhancement in the transmittance results, and shows the film removal mechanism. The protective DLC film adheres well to the substrate and does not peel under the blast. The film is thrown out with the material below when Hertz cracks form a pit. The exposed area seems to be less dark to the unaided eye, but it scatters the light and there is no enhancement in the specular reflectance and transmittance.

Protection of the DLC Films on Fused Silica

The protection of the DLC films on the substrate can be defined as the slope in figure 11. The lower the slope of the regression line, the longer the beadblast duration needed to get down to the specified transmittance. This means a longer useful lifetime for the sample as a part of an optical system with certain specifications. The velocity of the beads in the test is about 30 m/sec which is equal to that of strong winds. The technique can serve as a quantitative test for the protection of films on optical materials under sand storms, dusty winds, and other field conditions.

There are small differences in the protection factor extracted from the transmittance and reflectance data. Most of these differences, however, come from measurements of the uncoated fused silica. The relative specular reflec-

tance and transmittance in coated silica are very close to each other (figs. 9 and 10). The reason for this can be understood from figure 12. The roughness of the coated region is smaller and it is flat between pits. Therefore, the difference between reflectance and transmittance comes from the surface protrusion damage between the pits. The difference is enhanced due to the different laws of reflections and refractions, and their relations to the normal direction. If the transmittance and reflectance curves of the coated samples in figures 9 and 10 are plotted against the time scale, constricted by the protection factor, then they fall very close to the curves of bare fused silica. Thus, one can use the theory of optical degradation of bare fused silica subjected to beadblasting presented in the former sections. The amount of damage reduction, $F(v)$, caused by beadblasting, has to be further reduced by the protection factor, therefore reducing the effective K for the model calculations.

CONCLUSIONS

In this paper, the transmittance and reflectance of laser light on damaged fused silica and damaged, coated fused silica were measured. The damages were generated by beadblasting with spherical glass beads. The blast pressure was about 10^5 Pa and the bead velocity 30 m/sec. Some processes in the surface deterioration, beside Hertz cones cracks, were observed. Roughness measurements showed that parts of the surface are damaged before the material is thrown out. It is shown that brittle materials have residual damage in any impact of beadblasting and this damage accumulates until the surface removal of the substrate and the film occurs. Model calculations have shown the various stages of surface failure, incubation time, and material removal. The form of the surface damage seems to be a feature of the brittle material, but the damage dimension depends on the bead dimensions. The bead velocity affects the process through the residual damage of single impact which determines the time evolution of the damage.

The coating on fused silica diminishes the damages of surface protrusion, and material removal is delayed. The protection of the film could be expressed by extended time of useful optical performance. For limited regions of damage, this can be shown by the protection curve, which portrays the damage in the coated regions versus the damage in uncoated regions. The coated surface deterioration is very similar to that of uncoated fused silica surface and can be reproduced by similar theoretical expressions. The above technique is suitable to be used as a quantitative test for evaluating the protection of optical materials under field conditions.

ACKNOWLEDGMENTS

The author would like to thank to Bruce Banks and Mike Mirtich for very fruitful discussions and to Diane Swec for the SEM photographs.

REFERENCES

1. J.A. Zukas, "Impact Dynamics" (Wiley, New York, 1982).
2. D. Tabor, Ed., Proceeding of the Conference "Erosion by Liquid and Solid Impact" (Cambridge University, 1979).
3. D.G. Rickory and N.H. McMillan, "Wear of Materials, Eds., S.K. Rhee, A.W. Ruff, and K.C. Ludema, (American Soc. Engineers, New York, 1981).
4. W.F. Adler, Ed., "Erosion" (Amer. Soc. Materials Philadelphia, PA, 1979).
5. Marshall, et al. Wear 71 (1981), 363.
6. W.F. Adler, Wear 37 (1976), 353.
7. M.J. Mathewson, "Proc. 5th Int. Conf. on Ercsion" Ed. D. Tabor (Cambridge University, 1979).
8. M. El Sherbini and J. Halling, Wear 41 (1977), 365.
9. Ruff and Ives, Wear 35 (1975), 195.

ORIGINAL QUALITY
OF POOR QUALITY

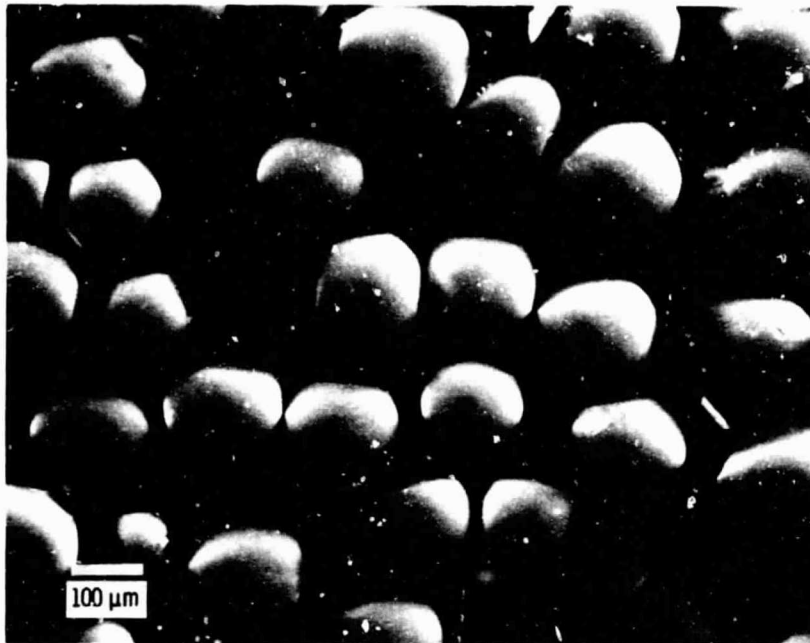


Figure 1. - SEM photograph of the spherical glass beads used for blasting.

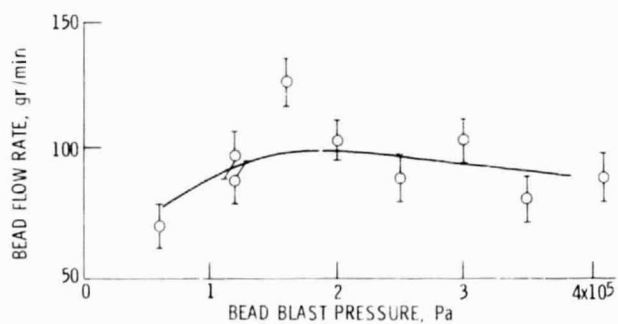


Figure 2. - Bead flow rate versus the bead-blast pressure. Only small dependence is observed.

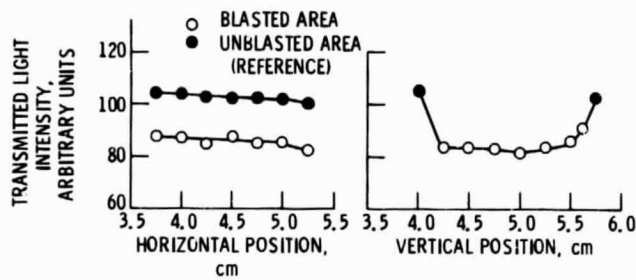


Figure 3. - Optical damage profile after the bead blasting of the fused silica slide. Transmittance through the damaged area is marked by circles and is almost independent of position.

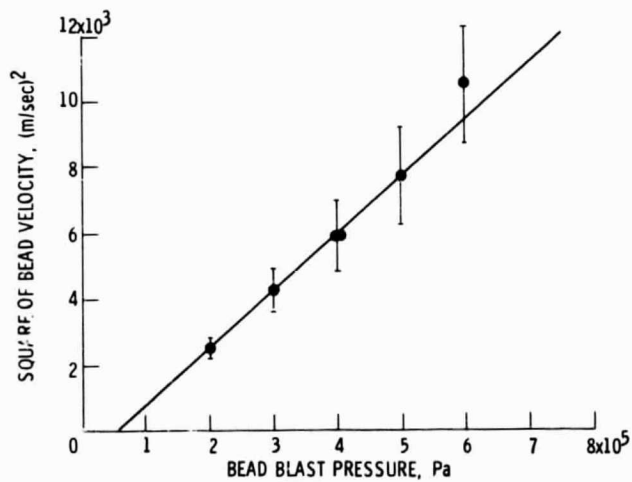


Figure 4. - Near linear dependence of square of bead velocity and bead blast pressure.

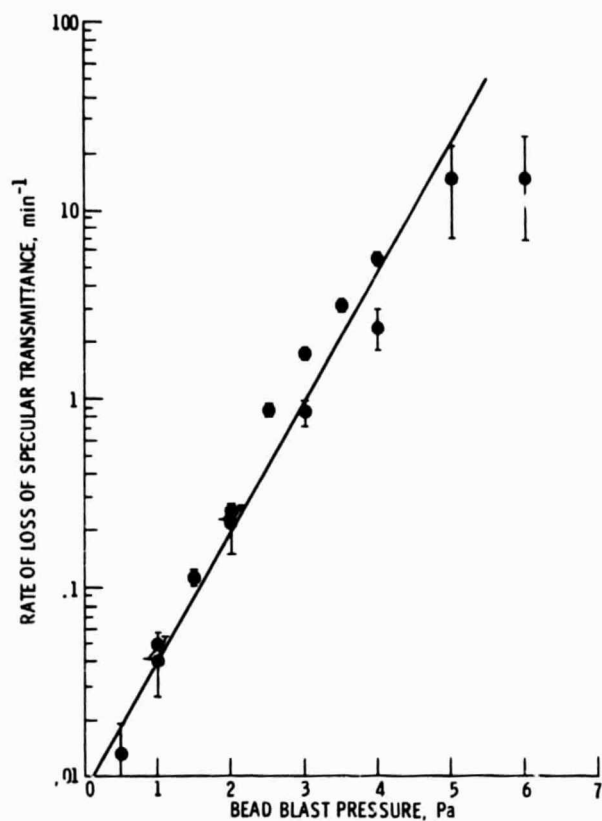


Figure 5. - Dependence of the rate of loss of specular transmittance on the bead blast pressure

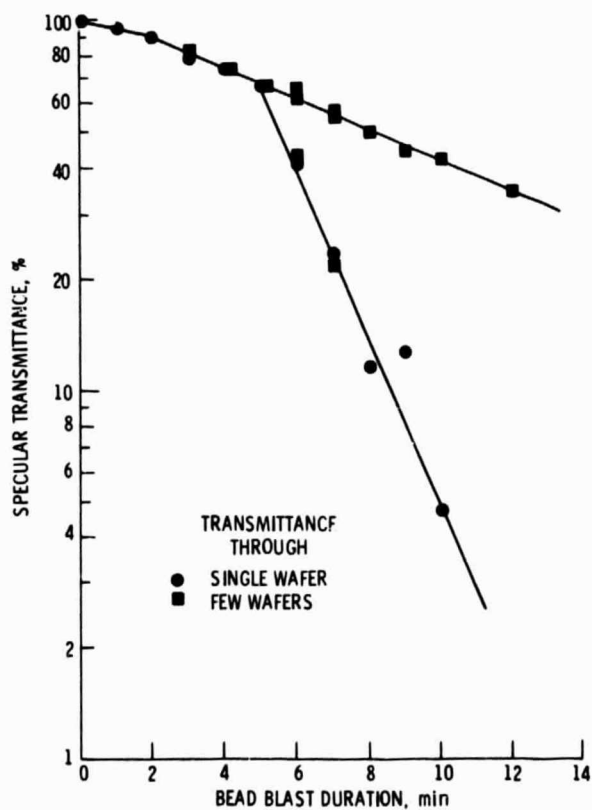


Figure 6. - Specular transmittance versus the bead-blast duration. Bead blasting pressure is 1.2×10^5 pascals. Transmittance through a few consecutive samples are plotted versus the combined bead blast duration for these samples.

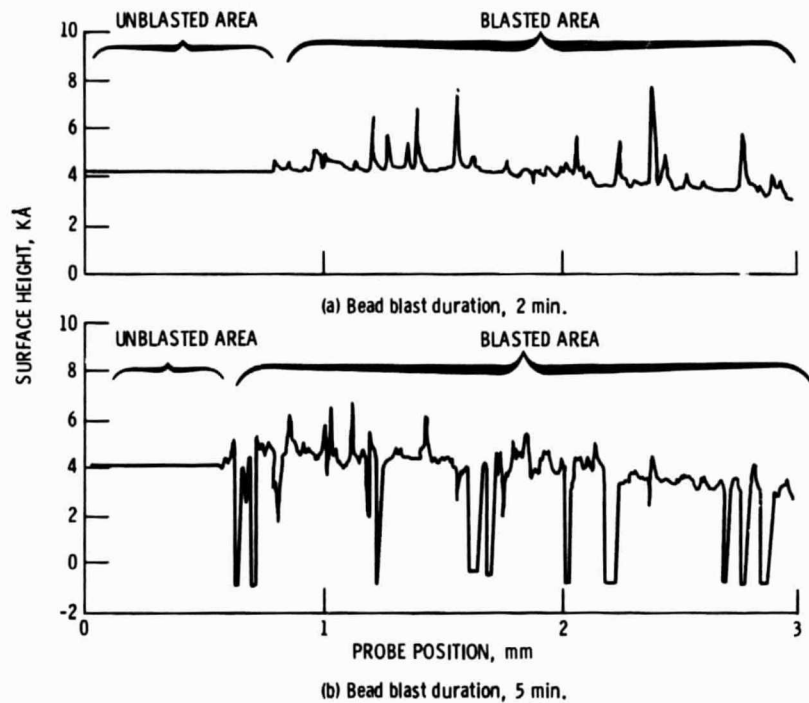
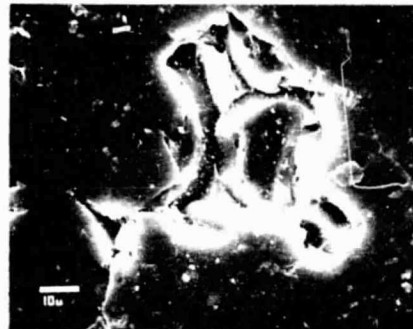
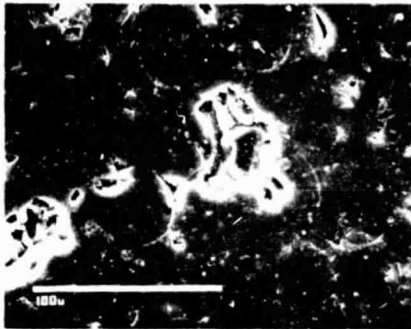
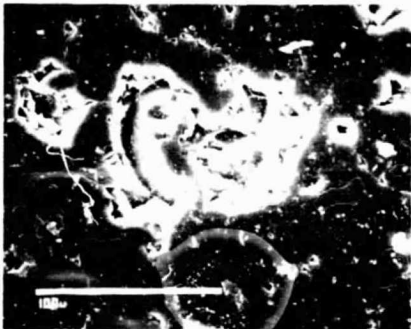


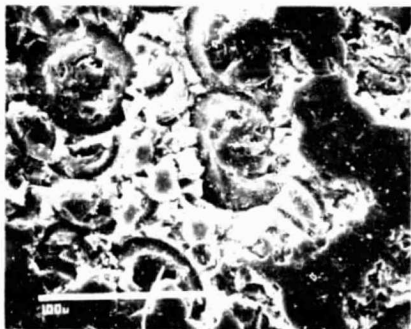
Figure 7. - Surface roughness as measured by profilometer at the end of the blasted region. Blasting pressure, 1.2×10^5 Pa.



(a) Blast duration 2 min.



(b) Blast duration 5 min.



(c) Blast duration 8 min; lower photograph was taken 30° off verticle.

Figure 8. - SEM photographs of samples after blasting. Note material thrown from a ring around the impacted area.

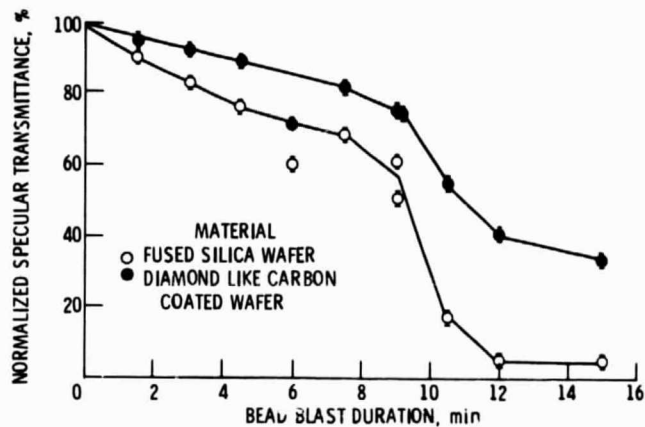


Figure 9. - Normalized specular transmittance of the blasted and un-blasted regions versus bead blast duration for a pressure of 10^5 Pa. The protection effect of the coating is demonstrated by higher transmittance.

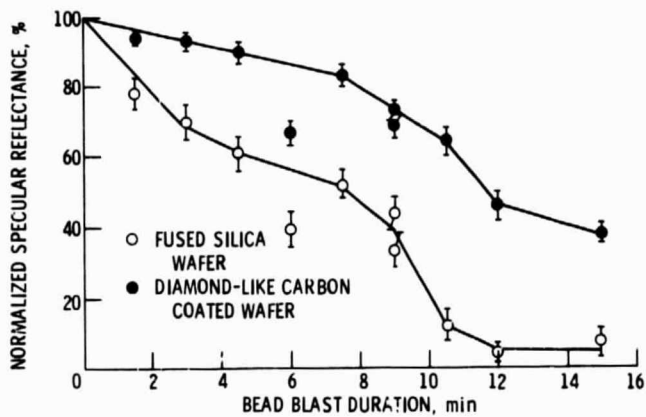


Figure 10. - Normalized specular reflectance of the blasted samples versus the beadblast duration. Protection effect is shown by the higher transmittance.

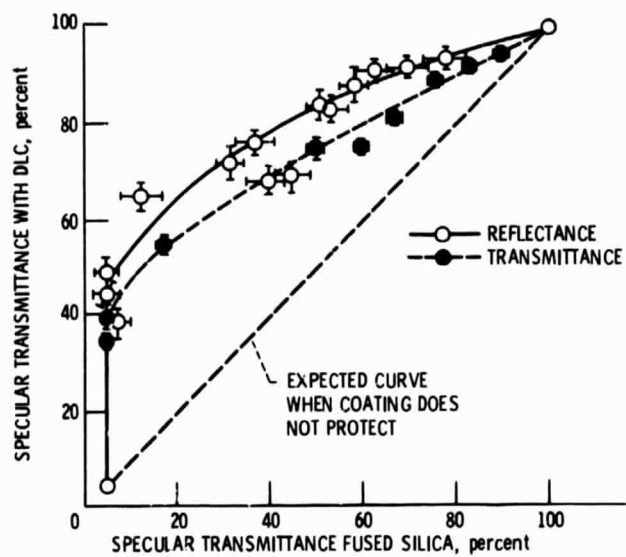


Figure 11. - Data of figures 9 and 10 when the normalized transmittance (reflectance) of the coated samples is plotted versus the transmittance (reflectance) of the uncoated fused silica.

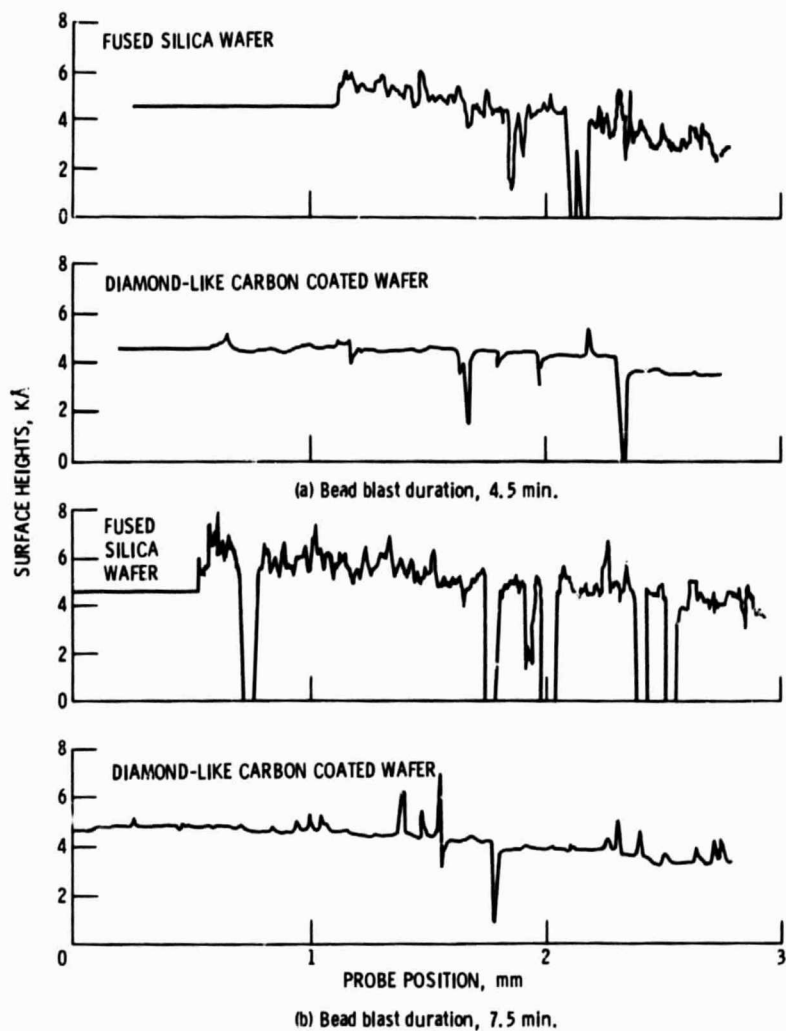


Figure 12. - Surface profiles of fused silica samples and of samples coated with 1000 \AA^0 DLC films. The profiles are different regions of the same samples. Protection effects are shown by the reduced roughness of the coated samples.

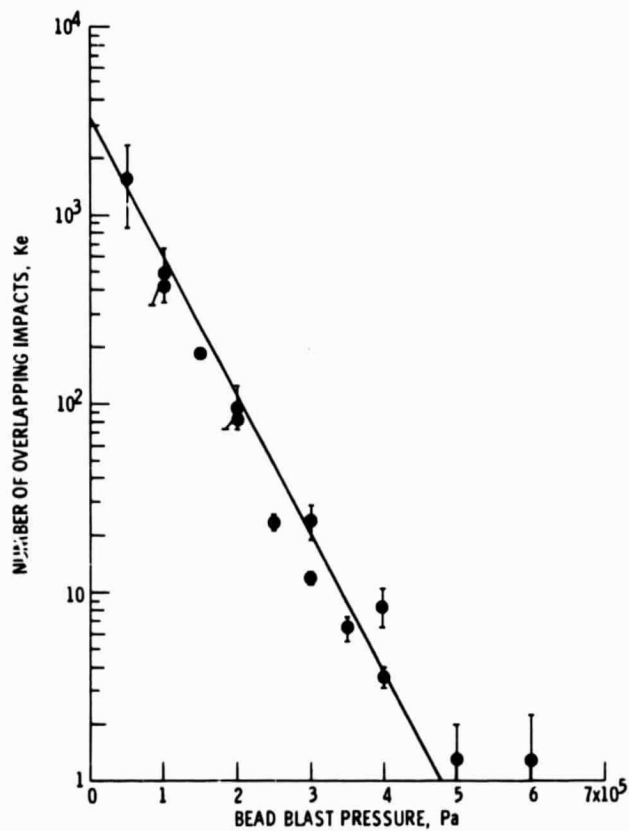


Figure 13. - Number of impacts overlapping on bombarded area $\pi R^2/4$ (where R is the bead radius) and causing 50% reduction in specular transmittance versus the beadblast pressure indicating a decreasing exponential dependence.

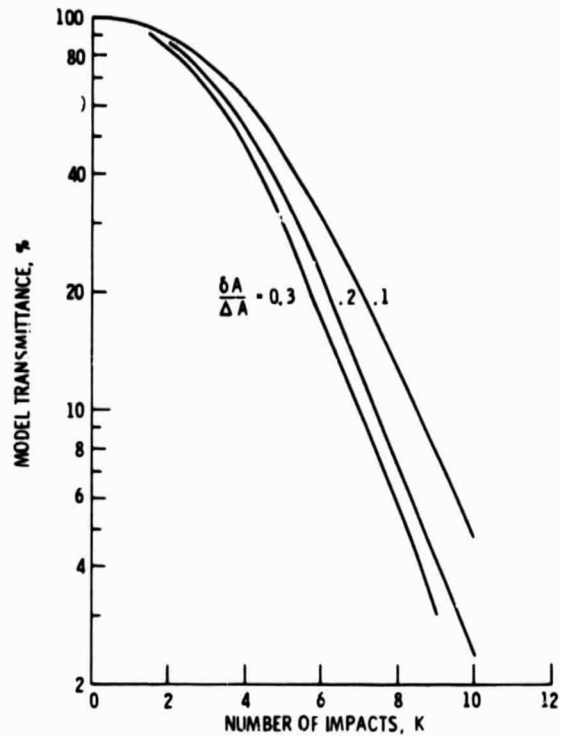


Figure 14. - Material throwing model: calculated transmittance of heavily damaged fused silica. The material is assumed to be thrown from an area δA when three cracks partially overlap. The transmittance is plotted versus the number of overlapping impacts on area ΔA , and every impact is assumed to cause a circular crack with dimension ΔA .

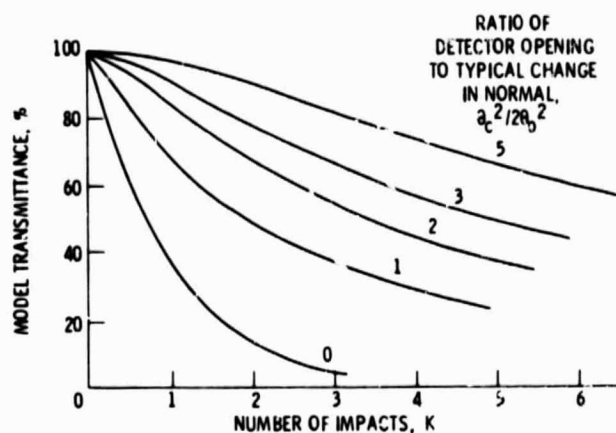


Figure 15. - Surface protrusion model: calculated transmittance of fused silica sample after a short duration and low pressure beadblast. The transmittance is plotted versus the number of overlapping impacts on a typical damage area ΔA . Every impact is assumed to cause some change in the surface normal direction.

1. Report No. NASA TM-87056		2. Government Accession No.		3. Recipient's Catalog No.	
4. Title and Subtitle Mechanical Protection of DLC Films on Fused Silica Slides				5. Report Date	
				6. Performing Organization Code 506-55-72	
7. Author(s) Dan N1r				8. Performing Organization Report No. E-2423	
				10. Work Unit No.	
9. Performing Organization Name and Address National Aeronautics and Space Administration Lewis Research Center Cleveland, Ohio 44135				11. Contract or Grant No.	
				13. Type of Report and Period Covered Technical Memorandum	
12. Sponsoring Agency Name and Address National Aeronautics and Space Administration Washington, D.C. 20546				14. Sponsoring Agency Code	
15. Supplementary Notes NRC-NASA Research Associate. Prepared for the 12th International Conference on Metallurgical Coatings, sponsored by the American Vacuum Society, Los Angeles, California, April 15-19, 1985.					
16. Abstract Measurements were made with a new test for improved quantitative estimation of the mechanical protection of thin films on optical materials. The mechanical damage was induced by a sand blasting system using spherical glass beads. Development of the surface damage was measured by the changes in the specular transmission and reflection, and by inspection using a surface profilometer and a scanning electron microscope. The changes in the transmittance versus the duration of sand blasting was measured for uncoated fused silica slides and coated ones. It has been determined that the diamondlike carbon films double the useful optical lifetime of the fused silica. Theoretical expressions were developed to describe the stages in surface deterioration. Conclusions were obtained for the SiO₂ surface removal mechanism and for the film removal mechanism.					
17. Key Words (Suggested by Author(s)) Bead blasting; Thin film; Protection; Diamondlike carbon film; Transmission reduction			18. Distribution Statement Unclassified - unlimited STAR Category 27		
19. Security Classif. (of this report) Unclassified		20. Security Classif. (of this page) Unclassified		21. No. of pages	
				22. Price*	